Molecular Pharmacology Fast Forward. Published on October 22, 2008 as DOI: 10.1124/mol.108.050492
Molecular Pharmacology Fast Forward. Published on October 22, 2008 as doi:10.1124/mol.108.050492
This article has not been copyedited and formatted. The final version may differ from this version.

Inhibition of P-Glycoprotein-Mediated Taxol Resistance by Reversibly-Linked Quinine Homodimers

Marcos M. Pires, Dana Emmert, Christine A. Hrycyna*, Jean Chmielewski*

From the Department of Chemistry and the Purdue Cancer Center, Purdue University,

West Lafayette, Indiana 47907-2084

Downloaded from molpharm.aspetjournals.org at ASPET Journals on April 16, 2024

Copyright 2008 by the American Society for Pharmacology and Experimental Therapeutics.

Molecular Pharmacology Fast Forward. Published on October 22, 2008 as DOI: 10.1124/mol.108.050492
This article has not been copyedited and formatted. The final version may differ from this version.

Running Title: Quinine-Dimer Inhibition of P-gp

Address correspondence to:

Jean Chmielewski, Ph.D. or Christine A. Hrycyna, Ph.D.

560 Oval Drive

West Lafayette, IN 47907-2084

Phone: 765-4940135

Fax: 765-4940239

E-mail: chml@purdue.edu; hrycyna@purdue.edu

Number of text pages: 31

Number of tables: 2

Number of figures: 8

Number of references: 40

Number of words in *Abstract*: 232

Number of words in *Introduction*: 696

Number of words in *Discussion*: 661

Abbreviations: P-gp, P-glycoprotein; MALDI-TOF, Matrix Assisted Laser Desorption Ionization - Time of Flight; ABC, ATP-Binding Cassette; PBS, Phosphate buffered saline; R123, Rhodamine 123; FACS, Flow Cytometry Cell Sorter; RPMI 1640 medium, Roswell Park Memorial Institute 1640 medium; Tris, tris(hydroxymethyl) aminomethane; 4-(2-Aminoethyl) benzenesulfonyl fluoride; DTT, Dithiothreitol.

Downloaded from molpharm.aspetjournals.org at ASPET Journals on April 16, 2024

Molecular Pharmacology Fast Forward. Published on October 22, 2008 as DOI: 10.1124/mol.108.050492
This article has not been copyedited and formatted. The final version may differ from this version.

ABSTRACT

P-glycoprotein (P-gp), an ATP-dependent drug efflux pump, has been implicated in multidrug resistance of several cancers due to its over-expression. Here rationally designed second-generation P-gp inhibitors are disclosed, based on dimerized versions of the substrates quinine and quinidine. These dimeric agents include reversible tethers with a built-in clearance mechanism. The designed agents were potent inhibitors of rhodamine 123 efflux in cultured cancer cell lines that display high levels of P-gp expression at the cell surface and in transfected cells expressing P-gp. The quinine homodimer Q2, which was tethered by reversible ester bonds, was particularly potent ($IC_{50} \approx 1.7$ μM). Further studies revealed that Q2 inhibited the efflux of a range of fluorescent substrates (rhodamine 123, doxorubicin, mitoxantrone, and Bodipy-FL-prazosin) from MCF-7/DX1 cells. The reversibility of the tether was confirmed in experiments showing that Q2 was readily hydrolyzed by esterases *in vitro* ($t_{1/2} \approx 20$ h), while demonstrating high resistance to non-enzymatic hydrolysis in cell culture media ($t_{1/2} \approx 21$ d). Specific inhibition of [^{125}I]-IAAP binding to P-gp by Q2 verified that the bivalent agent interacted specifically with the drug binding site(s) of P-gp. Q2 was also an inhibitor of verapamil-stimulated ATPase activity. Additionally, low concentrations of Q2 stimulated basal P-gp ATPase levels. Finally, Q2 was shown to inhibit the transport of radiolabeled taxol in MCF-7/DX1 cells and it completely reversed the P-gp mediated taxol-resistance phenotype.

Downloaded from molpharm.aspetjournals.org at ASPET Journals on April 16, 2024

Molecular Pharmacology Fast Forward. Published on October 22, 2008 as DOI: 10.1124/mol.108.050492
This article has not been copyedited and formatted. The final version may differ from this version.

INTRODUCTION

Small molecule drugs are integral parts of any cancer treatment. As such, the emergence of multidrug resistance threatens to undermine the use of a large number of effective anti-cancer agents. Most cancers are either intrinsically resistant to initial chemotherapy or acquire resistance over time (Ambudkar et al., 1999; Hrycyna, 2001). Previous studies have established that a broad-based drug resistance arises in large part from the over-expression of a plasma membrane polypeptide known as P-glycoprotein (P-gp) (Gottesman et al., 2002; Loscher and Potschka, 2005; Schinkel and Jonker, 2003). The endogenous expression of P-gp in the gut and blood brain barrier is an additional barrier that further restricts the bioavailability and brain penetration of chemo-agents.

P-gp is one of the most widely studied members of a large superfamily of ATP-dependent proteins known as ATP-Binding Cassette (ABC) transporters (Gottesman and Pastan, 1988; Higgins, 1992; Hrycyna, 2001). P-gp is an integral membrane protein comprised of two homologous halves each containing a cytosolic ATP binding site and six transmembrane segments. The binding of ATP and its subsequent hydrolysis are essential for the transport of P-gp substrates (Hrycyna et al., 1999; Loo and Clarke, 1995). P-gp uses the energy of ATP-hydrolysis to transport molecules and keep them out of cells, thereby limiting the intracellular concentration of drugs to levels that elicit little or no biological activity (Horio et al., 1988). The drug binding sites in P-gp have been previously shown to localize within the transmembrane segments, although the exact location within the protein where individual substrates bind is unknown due to the lack of a high resolution crystal structure (Ecker et al., 2002).

Downloaded from molpharm.aspetjournals.org at ASPET Journals on April 16, 2024

Molecular Pharmacology Fast Forward. Published on October 22, 2008 as DOI: 10.1124/mol.108.050492
This article has not been copyedited and formatted. The final version may differ from this version.

P-gp substrates encompass a wide range of structurally and functionally unrelated compounds. Examples of molecules effluxed by P-gp include: agents that possess anti-cancer activity such as taxol (Sparreboom et al., 1997), imatinib (Gleevec) (Illmer et al., 2004), and doxorubicin (Kartner et al., 1983); compounds that target HIV protease (Lee et al., 1998); the immunosuppressant cyclosporin A (Tsuji et al., 1993). Biochemical studies have revealed that there are at least two, if not more, distinct drug binding sites within the transmembrane regions of P-gp (Dey et al., 1997; Loo et al., 2003a; Loo et al., 2003b; Martin et al., 2000; Shapiro and Ling, 1997). Although cysteine cross-linking experiments (Loo et al., 2004) have pointed to a rotational symmetry of the two halves of P-gp (a pseudo 2-fold symmetry), the simultaneous binding of two different substrates has been shown to be feasible (Loo et al., 2003b). Combined, these studies suggest that P-gp likely has at least two distinct substrate binding sites.

Because the function of P-gp is non-essential for cellular homeostasis, reversible modulation of P-gp activity has been suggested to be an effective means of reversing multidrug resistance and increasing the bioavailability of drugs that are P-gp substrates. Previously, we demonstrated that by dimerizing the P-gp substrate emetine with an irreversible tether, potent inhibitors of P-gp could be generated (Pires et al., 2006). In this study, we sought to create a novel class of bivalent compounds that possess a mechanism of degradation that limits their persistence in the system. Here, we report the development of a class of bivalent inhibitors consisting of reversibly cross-linked P-gp substrates quinine and quinidine. These agents are capable of effectively inhibiting the transport activity of P-gp and reversing the taxol resistance phenotype of MCF-7/DX1cells. In addition, these inhibitors are based on inexpensive starting materials that

Downloaded from molpharm.aspetjournals.org at ASPET Journals on April 16, 2024

Molecular Pharmacology Fast Forward. Published on October 22, 2008 as DOI: 10.1124/mol.108.050492
This article has not been copyedited and formatted. The final version may differ from this version.

have been deemed safe for human use, and, therefore, may have further advantages over other P-gp inhibitors undergoing development.

Downloaded from molpharm.aspetjournals.org at ASPET Journals on April 16, 2024

Molecular Pharmacology Fast Forward. Published on October 22, 2008 as DOI: 10.1124/mol.108.050492
This article has not been copyedited and formatted. The final version may differ from this version.

MATERIALS AND METHODS

Materials. Quinine, quinidine, doxorubicin, mitoxantrone and cyclosporin A were purchased from Fluka (Switzerland). Rhodamine 123 and Bodipy-FL-prazosin were purchased from Molecular Probes, Inc. (Eugene, OR). [^{3}H]-Taxol and [^{125}I]-iodoarylazidoprazosin were purchased from Perkin Elmer Life and Analytical Sciences (Boston, MA). All other chemicals were purchased from Sigma-Aldrich (St. Louis, MO) and used without purification.

General Synthesis of Bivalent Quinine/Quinidine Compounds. To a solution of the commercially available tether (0.07 mmol) in dry dichloromethane (5 ml) at room temperature was added EDC (0.28 mmol), DMAP (0.03 mmol), and DIEA (0.28 mmol). After 20 min, quinine or quinidine (0.21 mmol) was added neat. The mixture was allowed to stir for 12 h at room temperature, and the solvent was removed *in vacuo*. The residue was dissolved in DMSO and filtered. The desired material was purified to homogeneity by reverse phase HPLC using a Vydac C8 column with an eluent consisting of solvent A (H_2O/0.1% TFA) and solvent B (CH_3CN/0.1% TFA) with a 60 min gradient consisting of 10 to 70% A, a flow rate of 8 ml/min, and monitoring at 214 and 280 nm. Each compound was characterized by MALDI-TOF mass spectrometry. **Q2** $[M+H]^+$: 815.47 (calculated) 815.06 (found), **1** $[M+H]^+$: 773.43 (calculated) 773.85 (found), **2** $[M+H]^+$: 829.40 (calculated) 829.86 (found), **3** $[M+H]^+$: 807.41 (calculated) 807.91 (found), **4** $[M+H]^+$: 792.02 (calculated) 791.87 (found), **5** $[M+H]^+$: 815.47 (calculated) 815.74 (found), **6** $[M+H]^+$: 815.47 (calculated) 816.00 (found).

Cell Culture. MCF-7 and MCF-7/DX1 cell lines were cultures at 37 °C with 5% CO_2. MCF-7 cells (breast adenocarcinoma) were cultured in RPMI 1640 medium

Downloaded from molpharm.aspetjournals.org at ASPET Journals on April 16, 2024

Molecular Pharmacology Fast Forward. Published on October 22, 2008 as DOI: 10.1124/mol.108.050492
This article has not been copyedited and formatted. The final version may differ from this version.

supplemented with 10% fetal bovine serum (Cambrex Bio Science Walkersville, Inc.), 2 mM L-glutamine (Cellgro, Mediatech), and 50 units/ml penicillin and 50 µg/ml streptomycin (Cellgro, Mediatech). The MCF-7/DX1 cell line over-expressing P-gp was maintained in the media above with the addition of 1 µM doxorubicin to the culture media. High Five cells were cultured at 27 °C in Express Five SFM medium (Gibco) supplemented with 18 mM L-glutamine (Cellgro, Mediatech) and 0.5X antibiotic-antimycotic (Gibco).

Flow Cytometry Assay. Substrate accumulation assays were performed as described previously with minor modifications (Hrycyna et al., 1998). For substrate accumulation studies using cell suspensions, 500,000 cells were incubated with either 1.3 µM rhodamine 123, 3 µM doxorubicin, 0.5 µM Bodipy-FL-prazosin alone or in the presence of varying concentrations of standard inhibitors or synthesized compounds for 30 min at 37 °C. For doxorubicin and prazosin, the cells were harvested by centrifugation at 300 *g* and resuspended in fresh media with or without inhibitor and incubated for an additional 30 min at 37 °C. The cells were harvested by centrifugation at 300 *g*, the media was removed, and the cells were resuspended in 400 µL of PBS. The cells were kept on ice until analysis. For rhodamine 123 assays performed in a 24 well plate, each well was evenly seeded and the cells were allowed to grow until they were 70-80% confluent and assayed under similar conditions except that the cells remained adhered to the plate. After the incubations, the cells were trypsized gently, resuspended in culture media and kept on ice until analysis. Cells were analyzed using a FACSCalibur flow cytometer (BD Biosciences, San Jose, CA) equipped with a 488-nm argon laser and a 530 band pass filter (FL1) for rhodamine 123. Ten thousand (10,000) cells were counted for each data

Downloaded from molpharm.aspetjournals.org at ASPET Journals on April 16, 2024

Molecular Pharmacology Fast Forward. Published on October 22, 2008 as DOI: 10.1124/mol.108.050492
This article has not been copyedited and formatted. The final version may differ from this version.

point. The fluorescence data were expressed as the mean of arbitrary fluorescence units derived from histogram plots of the 10,000 cells examined. All assays were performed in triplicate, and IC_{50} values were obtained by fitting the concentration dependent data using the program SigmaPlot (Systat, San Jose, CA).

Radioactive Substrate Accumulation Assay. Radioactive substrate accumulation assays were performed as described previously (Hrycyna et al., 1998) except that 6-well plates were used and seeded with 500,000 cells on the day prior to the assay. The next day, the media was removed and cells were washed 2X with cold PBS. Cells were then incubated with 2 ml of 7.5 nM [^{3}H]-taxol and increasing concentrations of **Q2** at 37 ºC for 40 min. Following this incubation, the media was removed and the cells were washed 2X with cold PBS. To each well, 1 ml of pre-warmed trypsin (37 ºC) was added and incubated at 37 ºC for 1 h. The entire contents of each well was placed in separate scintillation vials containing 18 mL EcoLite(+) scintillation fluid (MR Research Products, Irvine, CA). Each well was rinsed with an additional 500 µL of cold PBS (2X), added to the scintillation vial and counted using a scintillation counter. All assays were performed in triplicate, and IC_{50} values were obtained by fitting the concentration dependent data using the program SigmaPlot (Systat, San Jose, CA).

Expression of P-gp in High Five cells. High Five cells cultured in T75-cm^2 flasks (9.5 x 10^6 cells/flask) were infected with BV-*MDR*1 at a multiplicity of infection of 10 for 2 h at 27 °C in 2.5 ml culture medium as described previously (Germann et al., 1990). Following incubation for 2 h, 7.5 ml of media were added to the cells and incubated at 27 °C for 72 h.

Downloaded from molpharm.aspetjournals.org at ASPET Journals on April 16, 2024

Molecular Pharmacology Fast Forward. Published on October 22, 2008 as DOI: 10.1124/mol.108.050492
This article has not been copyedited and formatted. The final version may differ from this version.

Preparation of Crude High Five Membranes. BV-*MDR*1 infected High Five cells were harvested by sloughing off using a sterile Pasteur pipet 72 h post-infection and washed with phosphate-buffered saline (PBS), pH 7.4, supplemented with 1% (v/v) aprotinin. The cell pellet was resuspended at a density of 1 x 10^7 cells/ml in homogenization buffer containing 50 mM Tris (pH 7.5), 50 mM mannitol, 2 mM EGTA, 1 mM AEBSF, 2 mM DTT, and 1% (v/v) aprotinin. After 40 min incubation on ice, the cells were homogenized using 40 strokes with a dounce homogenizer (pestle A) and nuclear debris removed by centrifugation at 500*g* for 10 min. Crude membranes were isolated by centrifugation of the supernatant at 100,000*g* for 60 min at 4 °C and resuspended using blunt-ended 18, 20, 22 and 25-gauge needles sequentially in buffer containing 50 mM Tris (pH 7.5), 300 mM mannitol, 1 mM EGTA, 1 mM AEBSF, 1 mM DTT, 1% (v/v) aprotinin and 10% glycerol. The resuspended membranes were assayed for total protein concentration, frozen on dry ice in small aliquots and stored at -80 °C (Germann et al., 1990). MDR1 expression was confirmed by immunoblot with C219 primary antibody (1:4000).

ATPase Assay. Crude membranes derived from High Five cells expressing human P-glycoprotein were analyzed for both vanadate-sensitive basal and drug-stimulated ATP consumption in the absence and presence of increasing concentrations of **Q2**. Activity was measured by the colorimetric detection of inorganic phosphate released at 880 nm, as described previously (Hrycyna et al., 1998). Verapamil-stimulated activity was assayed in the presence of 30 μM verapamil plus or minus increasing concentrations of **Q2** using 10 μM cyclosporin A as a control inhibitor. All assays were performed in triplicate.

Downloaded from molpharm.aspetjournals.org at ASPET Journals on April 16, 2024

Molecular Pharmacology Fast Forward. Published on October 22, 2008 as DOI: 10.1124/mol.108.050492
This article has not been copyedited and formatted. The final version may differ from this version.

IAAP Photoaffinity Labeling. [^{125}I]-Iodoarylazidoprazosin ([^{125}I]-IAAP) (specific activity 2200 Ci/mmol) was used to label P-gp as described previously (Hrycyna et al., 1998). The reaction scale was reduced to a total volume of 40 μL. The crude membranes (25 μg) containing either DMSO or increasing concentrations of Q2 were incubated at room temperature in 50 mM Tris-HCl, pH 7.5, 2% aprotinin, 2 mM DTT and 4 mM AEBSF with IAAP (3 nM) for 10 min in the dark. The samples were then illuminated with a UV lamp assembly fitted with two black light UV-A long wave tubes (365 nm) for 20 minutes on ice. Membrane protein (20 μg) was subjected to SDS-PAGE on a 7.5% Tris glycine gel, fixed, dried overnight and exposed to Bio-Max MR film (Eastman Kodak Co.) at -80 °C for 12-24 h. To determine the amount of [^{125}I]-IAAP photocrosslinked to P-gp, each band was quantified using Image J (NIH, Bethesda, MD). Values were expressed either in arbitrary units or as percentages of a DMSO control experiment.

Confocal Microscopy. For confocal microscopy images, 20,000 cells were seeded onto Lab-Tek 4-well chamber slides on the day prior to the assay. Cells were then incubated with either 1.3 μM rhodamine 123, 10 μM doxorobucin, 10 μM mitoxantrone, or 250 nM Bodipy-FL-prazosin either alone or in the presence of synthesized compounds in RPMI 1640 media for 45 min at 37 °C. Images were acquired using a Radiance 2100 MP Rainbow (Bio-Rad, Hemel Hempstead, England) on a TE2000 (Nikon, Tokoyo, Japan) inverted microscope using a 60x oil 1.4 NA lens. Images were collected sequentially to avoid any possible bleed through. The mitoxantrone and doxorubicin were excited at 543 nm using the green HeNe laser and the fluorescence emission greater than 560 nm in wavelength was collected. Rhodamine 123 and Bodipy-FL-prazosin were excited with

Downloaded from molpharm.aspetjournals.org at ASPET Journals on April 16, 2024

Molecular Pharmacology Fast Forward. Published on October 22, 2008 as DOI: 10.1124/mol.108.050492
This article has not been copyedited and formatted. The final version may differ from this version.

the 488 nm line of the 4-line argon and the emission was collected with a 500LP, 550SP filter combination. A transmission image was also collected to show cell morphology.

Cell Viability Assay. For cell viability assays, 2,000 cells per well were plated onto Costar 96 well plates in 100 μL of cell media on the day prior to the assay. On the day of the assay, 100 μL of media was added to each well with varying concentrations of compound. Cells were incubated at 37 °C for 72 h. Following this incubation, 20 μL of a 5 mg/ml solution of MTT (3-(4,5-dimethylthiazol-2-yl)-2,5-diphenyltetrazolium bromide) was added to each well and incubated for 4 h at 37 °C (Mosmann, 1983). The media was carefully removed without disturbing the crystals formed on the bottom of the plates and 100 μL of dimethylsulfoxide was added to each well. The absorbance of the DMSO solution was measured at 590 nm and cell viability was calculated as a ratio of absorbance of the cells treated with synthetic compounds relative to untreated cells.

Porcine Liver Esterase Stability. Q2 was dissolved to a final concentration of 70 μM in RPMI 1640 (final DMSO concentration 0.35%). A total of 10 units of porcine liver esterase (EC 3.1.1.1, Sigma, St. Louis, MI) were added and the solution was placed in a 37 °C water bath (final concentration 10 units/ml). At different time points, aliquots from the reaction mixture were removed and immediately injected into the HPLC equipped with a Vydac C18 column with an eluent consisting of solvent A (H_2O/0.1% TFA) and solvent B (CH_3CN/0.1% TFA) with a 30 min gradient consisting of 5 to 50% A, a flow rate of 1 ml/min, and monitoring at 280 nm. The absorption at 250 nm was monitored and the peak area corresponding to **Q2** was quantified. The amount of **Q2** remaining intact was calculated from the initial peak area. All assays were performed in

Downloaded from molpharm.aspetjournals.org at ASPET Journals on April 16, 2024

Molecular Pharmacology Fast Forward. Published on October 22, 2008 as DOI: 10.1124/mol.108.050492
This article has not been copyedited and formatted. The final version may differ from this version.

triplicate, and half lives were obtained by fitting the time dependent data using the program SigmaPlot (Systat, San Jose, CA).

Downloaded from molpharm.aspetjournals.org at ASPET Journals on April 16, 2024

Molecular Pharmacology Fast Forward. Published on October 22, 2008 as DOI: 10.1124/mol.108.050492
This article has not been copyedited and formatted. The final version may differ from this version.

RESULTS

P-gp has been shown to simultaneously bind two or more distinct substrates (Dey et al., 1997; Loo et al., 2003a; Loo et al., 2003b; Martin et al., 2000; Shapiro and Ling, 1997). This multiplicity likely increases the overall efficiency of P-gp and facilitates the generation of a steep concentration gradient of substrates across plasma membranes of cells. However, it also provides the opportunity for the design of multivalent inhibitors and probes that interact with some or all of these discrete binding sites on P-gp.

We (Pires et al., 2006) and others (Chan et al., 2006; Sauna et al., 2004) have shown that irreversibly cross-linked homodimeric agents composed of P-gp substrates are potent P-gp inhibitors. To further illustrate the utility of this strategy, we set out to create a new class of reversibly cross-linked inhibitors composed of the P-gp substrates quinine and quinidine (Figure 2). The potency of these compounds should be greatly enhanced by increasing their effective concentration and their ability to bind to multiple drug binding sites in P-gp via an appropriately designed tether. Quinine and quinidine are transported by P-gp and also weakly modulate its transport activity (Wang et al., 2001). Both quinine and quinidine also have hydroxyl groups that can be conveniently esterified, thus providing an efficient route to dimeric molecules. Therefore these agents were chosen as our candidates for dimerization. The ester-based linkers used here were specifically chosen since they allow for the release the monomeric molecules once the dimeric agents reach the cytosol of cells. Ester bonds are known for being relatively stable under physiological conditions; however, they are ultimately broken down either through the action of non-enzymatic hydrolysis or by metabolic enzymes. Therefore, importantly, this strategy should yield novel inhibitors with low systemic persistence of the parent

Downloaded from molpharm.aspetjournals.org at ASPET Journals on April 16, 2024

Molecular Pharmacology Fast Forward. Published on October 22, 2008 as DOI: 10.1124/mol.108.050492
This article has not been copyedited and formatted. The final version may differ from this version.

compound. Both alkaloids were dimerized using spacers of different lengths, hydrophobicities, and flexibilities using the optimized tether from our previous study as a starting point.

A library approach was desirable since it generated a diverse set of molecules, thus increasing the likelihood of discovering potent and specific inhibitors of P-gp. The library described here consisted of quinine homodimers (**Q2** and **1-4**), a quinine/quinidine heterodimer (**5**), and a quinidine homodimer (**6**) (Figure 1). The quinine-based homodimers contained spacers of different lengths and rigidities in an attempt to probe the ideal spacing for P-gp binding. In particular, agents **5** and **6** were investigated in order to study the effect of inhibitor symmetry on P-gp activity. Both monomeric quinine and quinidine were converted to their dimeric forms using an EDC-mediated coupling reaction with various bis-acid tethers (Figure 1). All compounds were purified to homogeneity by reverse phase HPLC and analyzed by MALDI-TOF mass spectroscopy. The purity of each compound was confirmed using analytical reverse phase HPLC.

To assess the function of P-gp and the inhibitory potency of our synthetic bivalent agents, two human carcinoma lines were used. The MCF-7 human breast cancer parental cell line was used as a negative control because it does not express detectable levels of P-gp. A multidrug resistant subline derived from MCF-7 cells, MCF-7/DX1, was used because it is 200-fold more resistant to doxorubicin (Fairchild et al., 1987) and has been shown to express high levels of P-gp by immunoblot analysis (Ejendal and Hrycyna, 2005).

Initially, a rhodamine 123 (R123) accumulation assay was used to determine the effect of the monomeric and dimeric compounds on P-gp activity (Table 1). The use of a

Downloaded from molpharm.aspetjournals.org at ASPET Journals on April 16, 2024

Molecular Pharmacology Fast Forward. Published on October 22, 2008 as DOI: 10.1124/mol.108.050492
This article has not been copyedited and formatted. The final version may differ from this version.

small library of agents was useful in screening for effective spacers that were capable of spanning the drug binding sites of P-gp. Increased fluorescence in R123 treated MCF-7/DX1 cells is indicative of inhibition of P-gp transport. When MCF-7/DX1 cells were treated with the dimeric quinine and quinidine agents, a marked increase in R123 accumulation was observed, suggestive of inhibition of P-gp transport activity (Table 1 and Figure 2). Dimeric agents were much more effective in inhibiting P-gp than monomeric agents. In particular, the quinine dimer **Q2** (IC_{50} value of 1.7 μM) was over 60 times more potent than the quinine monomer (IC_{50} value of 103 μM) in its ability to restore the accumulation of R123 in resistant cells (Figure 2). To confirm that the observed activity was P-gp dependent, vaccinia virus transfected HeLa cells expressing human P-gp were similarly evaluated (Hrycyna 1998). Dose dependent reversal of R123 efflux was also observed (data not shown).

The stereochemistry of the substrates and the nature of the linkers appear to play a fairly important role in the ability of these bivalent compounds to inhibit P-gp transport activity. An increase in tether flexibility led to more potent dimeric inhibitors and an increase in tether length was also favorable (Table 1). Specifically, the quinine homodimer linked by an inflexible naphthalene tether (**2**), and the dimer containing the relatively more flexible benzyl tether (**3**), both of which are approximately equal in tether length, were 17 and 3 times less potent than **Q2**, respectively. It was also observed that the quinidine homodimer (**6**) was 3-fold less active than the quinine homodimer cross-linked with the same tether (**Q2**), while the quinine-quinidine heterodimer (**5**) was as potent as **Q2**. **Q2** was chosen for further study due the simplicity of its synthesis.

Downloaded from molpharm.aspetjournals.org at ASPET Journals on April 16, 2024

Molecular Pharmacology Fast Forward. Published on October 22, 2008 as DOI: 10.1124/mol.108.050492
This article has not been copyedited and formatted. The final version may differ from this version.

Furthermore, quinine has been shown to be safer and better tolerated than quinidine in humans (Grace and Camm, 1998; Olliaro and Taylor, 2003).

To verify that inhibition of P-gp efflux was not only specific for R123, the quinine homodimer, **Q2**, was further evaluated with other P-gp substrates including Bodipy-FL-prazosin, doxorubicin, and taxol. The intrinsic fluorescence levels of doxorubicin and a fluorescent analog of prazosin, Bodipy-FL-prazosin, were monitored to determine cellular accumulation. It was observed that **Q2** inhibited the efflux of doxorubicin from the resistant cancer cells, MCF-7/DX1, with an IC_{50} value of 1.9 ± 0.1 μM (Figure 2B). It was also found that **Q2** inhibited the efflux of Bodipy-FL-prazosin with a similar IC_{50} value of 2.0 ± 0.2 μM (Figure 2C). This result was notable because Bodipy-FL-prazosin, although also a P-gp substrate, is structurally distinct from R123 and may not occupy the same binding site on P-gp as R123 (Shapiro et al., 1999). Furthermore, the ability of **Q2** to inhibit P-gp mediated transport of radiolabeled taxol was determined (Figure 2D). **Q2** was found to effectively restore the accumulation of radiolabeled taxol in a concentration dependent manner ($IC_{50} \approx 3.6 \pm 0.2$ μM). This finding not only validated the fluorescence-based assays, but also indicated that **Q2** may reverse the resistance of a highly effective anti-cancer agent.

Confocal microscopy was next used to verify that P-gp substrates were accumulating in the intracellular space of MCF-7/DX1 cells when co-administered with **Q2**. Cells were incubated with various fluorescent P-gp substrates (R123, Bodipy-FL-prazosin, mitoxantrone, doxorubicin) in the presence and absence of 5 μM **Q2** (Figure 3). Fluorescence emission was minimal in resistant cells in the absence of **Q2** (top panel). However, upon incubation with 5 μM **Q2**, the cells became highly fluorescent (bottom

Downloaded from molpharm.aspetjournals.org at ASPET Journals on April 16, 2024

Molecular Pharmacology Fast Forward. Published on October 22, 2008 as DOI: 10.1124/mol.108.050492
This article has not been copyedited and formatted. The final version may differ from this version.

panel). These findings demonstrate that **Q2** is able to restore the accumulation of various P-gp substrates in cells expressing high levels of P-gp and that these substrates remain inside the cells.

The ultimate goal in designing our second-generation of bivalent inhibitors was to cross-link FDA-approved pharmaceutical agents with biodegradable spacers. Specifically, these reversible linkers should yield dimeric agents stable enough to interact with P-gp and their disassembly inside the cell would, in turn, re-generate molecules whose pharmacokinetic and pharmacodynamic parameters are well established. There are numerous examples of the use of ester linkages in therapeutics as fully reversible handles (Mizen and Burton, 1998). Esters linkages are degraded through chemical or enzyme-catalyzed hydrolysis reactions, such as hydrolysis by ubiquitous intracellular esterases.

Porcine liver esterase is commonly used as a model for enzymatic ester hydrolysis. Therefore, we used this enzyme to determine the stability of the ester bonds in **Q2**. The reaction was initiated by incubating **Q2** (70 μM) in RPMI 1640 cell culture media containing porcine liver esterase (10 units/ml) at 37 ºC and hydrolysis was monitored and quantified by reverse phase HPLC (Figure 4). It was observed that **Q2** had a half life of approximately 20 ± 2 h. A moderate hydrolysis rate was predicted due to the bulky nature of the hydroxyl groups on quinine. Non-enzymatic hydrolysis was also evaluated by incubating **Q2** in cell culture media at 37 ºC with no added porcine liver esterase. Under these conditions, **Q2** was observed to have high stability in the assay media with a half-life in the order of weeks (21 ± 3 d), an indication that the ester bond is stable to serum and chemical hydrolysis (data not shown). These results suggest that **Q2** is likely

Downloaded from molpharm.aspetjournals.org at ASPET Journals on April 16, 2024

Molecular Pharmacology Fast Forward. Published on October 22, 2008 as DOI: 10.1124/mol.108.050492
This article has not been copyedited and formatted. The final version may differ from this version.

to remain intact in cell culture assays and should only be degraded following intracellular accumulation.

Q2 was designed to interact with the drug binding sites on P-gp and, therefore, it should also compete with other substrates for these binding sites. To verify that this homodimeric quinine inhibitor was binding to the drug binding region of P-gp, photo-affinity crosslinking experiments were performed with an I^{125} radiolabeled, azido-analog of prazosin ([^{125}I]IAAP) (Figure 5). Treatment of crude High Five membranes expressing P-gp with [^{125}I]IAAP, followed by photocrosslinking, led to the detection of a radiolabeled band on a polyacrylamide gel at the molecular weight corresponding to P-gp, indicating covalent modification of P-gp with IAAP. Co-incubation of P-gp with IAAP and increasing amounts of **Q2** was found to inhibit the incorporation of IAAP in a concentration dependent manner with an IC_{50} value of 150 ± 13 nM. Moreover, **Q2** appears to have a much higher affinity for P-gp than the monomeric quinine, as quinine failed to inhibit [^{125}I]IAAP labeling of P-gp up to 20 μM. These data are consistent with a previous study in which 100 μM of quinine was required to effectively inhibit the labeling of P-gp with a photoaffinity analog of vinblastine, (Akiyama et al., 1988). The finding that **Q2** blocks the drug binding site of prazosin with such a low IC_{50} implies there is a synergistic effect in affinity of **Q2** by dimerizing the substrate quinine.

The ATPase activity of P-gp is highly correlated with its transport activity (Horio et al., 1988). To assess this activity, crude membrane vesicles were prepared from High Five insect cells expressing human P-gp. The basal and drug-stimulated ATPase activities of P-gp were measured using both Q2 at various concentrations and verapamil (30 μM), a known P-gp substrate. The membrane vesicles were incubated with increasing

Downloaded from molpharm.aspetjournals.org at ASPET Journals on April 16, 2024

Molecular Pharmacology Fast Forward. Published on October 22, 2008 as DOI: 10.1124/mol.108.050492
This article has not been copyedited and formatted. The final version may differ from this version.

concentrations of **Q2** and ATPase activity was analyzed by measuring the amount of liberated inorganic phosphate using a spectrophotometer. While Q2 stimulated the basal ATPase activity of P-gp at low concentrations, the level of ATPase activity was unaffected at higher concentrations (Figure 6A). This specific ATPase stimulation behavior has been previously observed for other P-gp substrates and inhibitors (Ambudkar 1999). The monomeric quinine (25 μM) in the same experiment caused a modest stimulation of ATPase activity. It was observed that **Q2** inhibited the verapamil-stimulated ATPase activity of P-gp in a concentration dependent manner (Figure 6B). In contrast, incubation of monomeric quinine (25 μM) with the same membranes had little effect on verapamil-stimulated ATPase activity. These data demonstrate that **Q2** interferes with the verapamil-stimulated ATPase cycle of P-gp more effectively than monomeric quinine.

The P-gp-mediated multidrug resistance phenotype of cancer cells is characterized by the ability of cells to evade the cytotoxic effects of drugs that are substrates of P-gp and remain viable even at high extracellular drugs concentrations. One such compound is the cytostatic agent taxol, which is also a known P-gp substrate (Horwitz et al., 1993). Cells lines that over-express P-gp, such as the MCF-7/DX1 cell line, display a 3000-fold decrease in susceptibility to taxol (Table 2). The ability of **Q2** to reverse the resistance to taxol in these cells was evaluated using the MTT cell viability assay. In these experiments, MCF-7/DX1 cells were co-incubated with taxol and increasing concentrations of **Q2** for 72 h. An approximate 4.5-fold decrease in resistance to taxol was observed when cells were incubated with 2 μM of **Q2** (Figure 7A), and when taxol was co-incubated with 4 μM of **Q2**, the potency of taxol was equivalent to that of

Downloaded from molpharm.aspetjournals.org at ASPET Journals on April 16, 2024

Molecular Pharmacology Fast Forward. Published on October 22, 2008 as DOI: 10.1124/mol.108.050492
This article has not been copyedited and formatted. The final version may differ from this version.

the non-resistant parental cell line. These results indicated that 4 μM of **Q2** is sufficient to fully reverse the taxol-resistant phenotype of these cells. Co-incubation of higher concentrations of **Q2** (6 μM) had no additional effect on the IC_{50} value of taxol. Together, these data demonstrated that low micromolar levels of **Q2** led to a 3000-fold increase in potentiation of taxol cytotoxicity, thus completely reversing the resistance phenotype MCF-7/DX1 cells. The IC_{50} value for **Q2** alone was found to be 18 μM, a value that is higher than the effective concentration with taxol (Figure 7B).

Downloaded from molpharm.aspetjournals.org at ASPET Journals on April 16, 2024

Molecular Pharmacology Fast Forward. Published on October 22, 2008 as DOI: 10.1124/mol.108.050492
This article has not been copyedited and formatted. The final version may differ from this version.

DISCUSSION

A library of reversibly linked dimeric agents composed of quinine and quinidine monomers was used to identify inhibitors of P-gp. These agents were used in these studies because both are known substrates of P-gp and each have a hydroxyl-group available for easy modification to dimer. Results from a R123 accumulation assay screen using this library demonstrated that flexible tethers were more effective spacers than rigid tethers, and that a tether length of approximately 10 Å was sufficient to generate potent homodimeric inhibitors of P-gp (Table 1). Stereoselective interaction of P-gp with its substrates has been previously reported for the diastereomers of propranolol (Wigler and Patterson, 1994) and thioxanthenes (Ford et al., 1990). Differences in potency with the dimeric agents were also noted based on stereochemistry. For example, the quinine dimer **Q2** was a 3-fold more potent inhibitor of P-gp compared to the identically tethered quinidine agent (**6**). This difference in potency was lost, however, when a heterodimer of quinine and quinidine (**5**) was evaluated. Because the derivatization on the monomeric substrates quinine and quinidine occurs on the hydroxyl group that is part of the stereocenter that distinguishes these two diastereomers, it is possible that the tether is affecting the ability of these compounds to interact with the binding sites of P-gp. The hydroxyl on quinine in its P-gp bound state may be more exposed to the central core of P-gp than quinidine. Therefore, its modification may have little effect on how the remainder of the compound binds to P-gp.

The most potent quinine homodimer inhibitor from the library of reversibly tethered dimeric compounds, **Q2**, was found to inhibit the efflux of a wide range of substrates (R123, doxorubicin, Bodipy-FL-prazosin, taxol, and mitoxantrone) using a

Downloaded from molpharm.aspetjournals.org at ASPET Journals on April 16, 2024

Molecular Pharmacology Fast Forward. Published on October 22, 2008 as DOI: 10.1124/mol.108.050492
This article has not been copyedited and formatted. The final version may differ from this version.

number of parallel assays, including cellular efflux measurements, confocal microscopy, photo-affinity labeling, and analyses of ATPase activity. Significantly, the competitive photo-affinity labeling experiment indicated that **Q2** can effectively compete for the transporter binding sites normally occupied by the substrate prazosin. Although the heterodimeric compound (**5**) was equipotent with **Q2**, the better tolerability of the monomeric quinine and the ease of synthesis made **Q2** the more desireable of the two agents. Furthermore, the fact that the hydrolytic degradation of (**5**) releases two distinct therapeutic agents could potentially lead to unwanted drug-drug interactions.

It was envisioned that the **Q2** dimer would revert back to monomers once internalized into cells due to the esterase-labile bonds tethering quinine. The expected intracellular disassembly of **Q2** is quite desirable, as there should be a decrease in the extended persistence of these molecules in the system. **Q2** was found to be stable in cell culture media, with minimal breakdown observed after several days. On the other hand, **Q2** was found to be slowly ($t_{1/2} \approx 20$ h), but effectively hydrolyzed by porcine liver esterases. These kinetic profiles are consistent with our findings that **Q2** can inhibit P-gp during prolonged incubation assays, even in the presence of serum.

The most remarkable feature of the data presented is the reversal of taxol resistance in P-gp expressing cells by **Q2**. Taxol is a potent cytostatic drug but its effectiveness against cancer cell lines that display a high level of P-gp expression is significantly decreased. Upon the co-incubation of MCF-7/DX1 cells with taxol and **Q2**, it was found that the IC_{50} value of taxol was enhanced 3000-fold and returned to similar levels as non-resistant cells, thereby abolishing the multidrug resitance phenotype. **Q2** itself, by comparison, is not cytotoxic at these inhibitory concentrations. These data are

Downloaded from molpharm.aspetjournals.org at ASPET Journals on April 16, 2024

Molecular Pharmacology Fast Forward. Published on October 22, 2008 as DOI: 10.1124/mol.108.050492
This article has not been copyedited and formatted. The final version may differ from this version.

quite significant as the quinine dimers are extremely easy to prepare and are very inexpensive agents based on a commonly used starting material.

In conclusion, a novel class of reversibly-linked homodimeric P-gp inhibitors based on quinine and quinidine was designed and synthesized. A potent member of this library, **Q2**, was shown to act specifically on P-gp by inhibiting its transport activity. The finding that **Q2** was able to restore the potency of taxol against resistant cancer cells makes it a promising lead in the search for novel specific modulators of P-gp. Future plans include the expansion of this dimeric cross-linking strategy to other P-gp substrates with the goal of developing new agents that can act both as inhibitors of P-gp and therapeutic prodrugs. Additional ABC transporters may also be effectively inhibited with dimeric agents of the type described within, and these studies will be the focus of future experiments.

Downloaded from molpharm.aspetjournals.org at ASPET Journals on April 16, 2024

Molecular Pharmacology Fast Forward. Published on October 22, 2008 as DOI: 10.1124/mol.108.050492
This article has not been copyedited and formatted. The final version may differ from this version.

REFERENCES

Akiyama S, Cornwell MM, Kuwano M, Pastan I and Gottesman MM (1988) Most drugs that reverse multidrug resistance also inhibit photoaffinity labeling of P-glycoprotein by a vinblastine analog. *Mol Pharmacol* **33**(2):144-147.

Ambudkar SV, Dey S, Hrycyna CA, Ramachandra M, Pastan I and Gottesman MM (1999) Biochemical, cellular, and pharmacological aspects of the multidrug transporter. *Annu Rev Pharmacol Toxicol* **39**:361-398.

Chan KF, Zhao Y, Burkett BA, Wong IL, Chow LM and Chan TH (2006) Flavonoid dimers as bivalent modulators for P-glycoprotein-based multidrug resistance: synthetic apigenin homodimers linked with defined-length poly(ethylene glycol) spacers increase drug retention and enhance chemosensitivity in resistant cancer cells. *J Med Chem* **49**(23):6742-6759.

Dey S, Ramachandra M, Pastan I, Gottesman MM and Ambudkar SV (1997) Evidence for two nonidentical drug-interaction sites in the human P-glycoprotein. *Proc Natl Acad Sci U S A* **94**(20):10594-10599.

Ecker GF, Csaszar E, Kopp S, Plagens B, Holzer W, Ernst W and Chiba P (2002) Identification of ligand-binding regions of P-glycoprotein by activated-pharmacophore photoaffinity labeling and matrix-assisted laser desorption/ionization-time-of-flight mass spectrometry. *Mol Pharmacol* **61**(3):637-648.

Ejendal KF and Hrycyna CA (2005) Differential sensitivities of the human ATP-binding cassette transporters ABCG2 and P-glycoprotein to cyclosporin A. *Mol Pharmacol* **67**(3):902-911.

Downloaded from molpharm.aspetjournals.org at ASPET Journals on April 16, 2024

Molecular Pharmacology Fast Forward. Published on October 22, 2008 as DOI: 10.1124/mol.108.050492
This article has not been copyedited and formatted. The final version may differ from this version.

Fairchild CR, Ivy SP, Kao-Shan CS, Whang-Peng J, Rosen N, Israel MA, Melera PW, Cowan KH and Goldsmith ME (1987) Isolation of amplified and overexpressed DNA sequences from adriamycin-resistant human breast cancer cells. *Cancer Res* **47**(19):5141-5148.

Ford JM, Bruggemann EP, Pastan I, Gottesman MM and Hait WN (1990) Cellular and biochemical characterization of thioxanthenes for reversal of multidrug resistance in human and murine cell lines. *Cancer Res* **50**(6):1748-1756.

Germann UA, Willingham MC, Pastan I and Gottesman MM (1990) Expression of the human multidrug transporter in insect cells by a recombinant baculovirus. *Biochemistry* **29**(9):2295-2303.

Gottesman MM, Fojo T and Bates SE (2002) Multidrug resistance in cancer: role of ATP-dependent transporters. *Nat Rev Cancer* **2**(1):48-58.

Gottesman MM and Pastan I (1988) The multidrug transporter, a double-edged sword. *J Biol Chem* **263**(25):12163-12166.

Grace AA and Camm AJ (1998) Quinidine. *N Engl J Med* **338**(1):35-45.

Higgins CF (1992) ABC transporters: from microorganisms to man. *Annu Rev Cell Biol* **8**:67-113.

Horio M, Gottesman MM and Pastan I (1988) ATP-dependent transport of vinblastine in vesicles from human multidrug-resistant cells. *Proc Natl Acad Sci U S A* **85**(10):3580-3584.

Horwitz SB, Cohen D, Rao S, Ringel I, Shen HJ and Yang CP (1993) Taxol: mechanisms of action and resistance. *J Natl Cancer Inst Monogr*(15):55-61.

Downloaded from molpharm.aspetjournals.org at ASPET Journals on April 16, 2024

Molecular Pharmacology Fast Forward. Published on October 22, 2008 as DOI: 10.1124/mol.108.050492
This article has not been copyedited and formatted. The final version may differ from this version.

Hrycyna CA (2001) Molecular genetic analysis and biochemical characterization of mammalian P-glycoproteins involved in multidrug resistance. *Semin Cell Dev Biol* **12**(3):247-256.

Hrycyna CA, Ramachandra M, Germann UA, Cheng PW, Pastan I and Gottesman MM (1999) Both ATP sites of human P-glycoprotein are essential but not symmetric. *Biochemistry* **38**(42):13887-13899.

Hrycyna CA, Ramachandra M, Pastan I and Gottesman MM (1998) Functional expression of human P-glycoprotein from plasmids using vaccinia virus-bacteriophage T7 RNA polymerase system. *Methods Enzymol* **292**:456-473.

Illmer T, Schaich M, Platzbecker U, Freiberg-Richter J, Oelschlagel U, von Bonin M, Pursche S, Bergemann T, Ehninger G and Schleyer E (2004) P-glycoprotein-mediated drug efflux is a resistance mechanism of chronic myelogenous leukemia cells to treatment with imatinib mesylate. *Leukemia* **18**(3):401-408.

Kartner N, Shales M, Riordan JR and Ling V (1983) Daunorubicin-resistant Chinese hamster ovary cells expressing multidrug resistance and a cell-surface P-glycoprotein. *Cancer Res* **43**(9):4413-4419.

Lee CG, Gottesman MM, Cardarelli CO, Ramachandra M, Jeang KT, Ambudkar SV, Pastan I and Dey S (1998) HIV-1 protease inhibitors are substrates for the MDR1 multidrug transporter. *Biochemistry* **37**(11):3594-3601.

Loo TW, Bartlett MC and Clarke DM (2003a) Methanethiosulfonate derivatives of rhodamine and verapamil activate human P-glycoprotein at different sites. *J Biol Chem* **278**(50):50136-50141.

Downloaded from molpharm.aspetjournals.org at ASPET Journals on April 16, 2024

Molecular Pharmacology Fast Forward. Published on October 22, 2008 as DOI: 10.1124/mol.108.050492
This article has not been copyedited and formatted. The final version may differ from this version.

Loo TW, Bartlett MC and Clarke DM (2003b) Simultaneous binding of two different drugs in the binding pocket of the human multidrug resistance P-glycoprotein. *J Biol Chem* **278**(41):39706-39710.

Loo TW, Bartlett MC and Clarke DM (2004) Val133 and Cys137 in transmembrane segment 2 are close to Arg935 and Gly939 in transmembrane segment 11 of human P-glycoprotein. *J Biol Chem* **279**(18):18232-18238.

Loo TW and Clarke DM (1995) Covalent modification of human P-glycoprotein mutants containing a single cysteine in either nucleotide-binding fold abolishes drug-stimulated ATPase activity. *J Biol Chem* **270**(39):22957-22961.

Loscher W and Potschka H (2005) Drug resistance in brain diseases and the role of drug efflux transporters. *Nat Rev Neurosci* **6**(8):591-602.

Martin C, Berridge G, Higgins CF, Mistry P, Charlton P and Callaghan R (2000) Communication between multiple drug binding sites on P-glycoprotein. *Mol Pharmacol* **58**(3):624-632.

Mizen L and Burton G (1998) The use of esters as prodrugs for oral delivery of beta-lactam antibiotics. *Pharm Biotechnol* **11**:345-365.

Mosmann T (1983) Rapid colorimetric assay for cellular growth and survival: application to proliferation and cytotoxicity assays. *J Immunol Methods* **65**(1-2):55-63.

Olliaro PL and Taylor WR (2003) Antimalarial compounds: from bench to bedside. *J Exp Biol* **206**(Pt 21):3753-3759.

Pires MM, Hrycyna CA and Chmielewski J (2006) Bivalent probes of the human multidrug transporter P-glycoprotein. *Biochemistry* **45**(38):11695-11702.

Downloaded from molpharm.aspetjournals.org at ASPET Journals on April 16, 2024

Molecular Pharmacology Fast Forward. Published on October 22, 2008 as DOI: 10.1124/mol.108.050492
This article has not been copyedited and formatted. The final version may differ from this version.

R TB, Jeffrey A, Siahaan TJ, Gangwar S and Pauletti GM (1997) Improvement of oral peptide bioavailability: Peptidomimetics and prodrug strategies. *Adv Drug Deliv Rev* **27**(2-3):235-256.

Sauna ZE, Andrus MB, Turner TM and Ambudkar SV (2004) Biochemical basis of polyvalency as a strategy for enhancing the efficacy of P-glycoprotein (ABCB1) modulators: stipiamide homodimers separated with defined-length spacers reverse drug efflux with greater efficacy. *Biochemistry* **43**(8):2262-2271.

Schinkel AH and Jonker JW (2003) Mammalian drug efflux transporters of the ATP binding cassette (ABC) family: an overview. *Adv Drug Deliv Rev* **55**(1):3-29.

Shapiro AB, Fox K, Lam P and Ling V (1999) Stimulation of P-glycoprotein-mediated drug transport by prazosin and progesterone. Evidence for a third drug-binding site. *Eur J Biochem* **259**(3):841-850.

Shapiro AB and Ling V (1997) Positively cooperative sites for drug transport by P-glycoprotein with distinct drug specificities. *Eur J Biochem* **250**(1):130-137.

Sparreboom A, van Asperen J, Mayer U, Schinkel AH, Smit JW, Meijer DK, Borst P, Nooijen WJ, Beijnen JH and van Tellingen O (1997) Limited oral bioavailability and active epithelial excretion of paclitaxel (Taxol) caused by P-glycoprotein in the intestine. *Proc Natl Acad Sci U S A* **94**(5):2031-2035.

Tsuji A, Tamai I, Sakata A, Tenda Y and Terasaki T (1993) Restricted transport of cyclosporin A across the blood-brain barrier by a multidrug transporter, P-glycoprotein. *Biochem Pharmacol* **46**(6):1096-1099.

Downloaded from molpharm.aspetjournals.org at ASPET Journals on April 16, 2024

Molecular Pharmacology Fast Forward. Published on October 22, 2008 as DOI: 10.1124/mol.108.050492
This article has not been copyedited and formatted. The final version may differ from this version.

Wang EJ, Casciano CN, Clement RP and Johnson WW (2001) Active transport of fluorescent P-glycoprotein substrates: evaluation as markers and interaction with inhibitors. *Biochem Biophys Res Commun* **289**(2):580-585.

Wigler PW and Patterson FK (1994) Reversal agent inhibition of the multidrug resistance pump in human leukemic lymphoblasts. *Biochim Biophys Acta* **1189**(1):1-6.

Downloaded from molpharm.aspetjournals.org at ASPET Journals on April 16, 2024

Molecular Pharmacology Fast Forward. Published on October 22, 2008 as DOI: 10.1124/mol.108.050492
This article has not been copyedited and formatted. The final version may differ from this version.

FOOTNOTES

* The work was supported by NIH Grant (EY018481) and the Purdue Research Foundation. Microscopy data were acquired in the Purdue Cancer Center Analytical Cytometry Laboratories supported by the Cancer Center NCI core grant # NIH NCI-2P30CA23168.

Downloaded from molpharm.aspetjournals.org at ASPET Journals on April 16, 2024

Molecular Pharmacology Fast Forward. Published on October 22, 2008 as DOI: 10.1124/mol.108.050492
This article has not been copyedited and formatted. The final version may differ from this version.

Figure Legends

Figure 1. (A) Chemical structure of quinine and quinidine. (B) Representative synthetic scheme of the bivalent quinine and quinidine molecules. (C) Quinine and quinidine-based homodimeric and quinine/quinidine heterodimeric compounds investigated.

Figure 2. Concentration-dependent inhibitory potency of **Q2** on the transport of different P-gp substrates using MCF-7/DX1 cells. (A-C) MCF-7/DX1 cells were treated with R123 (1.3 μM), doxorubicin (3 μM), or Bodipy-FL-prazosin (0.5 μM) and various concentrations of inhibitors for 30 min at 37 ºC, then in drug-free media for 30 min at 37 ºC. Cells were analyzed for fluorescence using a FACSCalibur flow cytometer. (D) MCF-7/DX1 cells were treated with [^{3}H]-taxol (7.5 nM) and various concentrations of **Q2** for 40 min at 37 ºC, then with trypsin for 1 h at 37 ºC. Cells were analyzed for accumulation of the radioactive taxol using a scintillation counter.

Figure 3. Confocal microscopy images of MCF-7/DX1 cells incubated with various fluorescent substrates of P-gp in the presence and absence of **Q2**. Cells were incubated for 45 min at 37 °C with 1.3 μM R123, 10 μM mitoxantrone, 10 μM doxorobucin, or 250 nM Bodipy-FL-prazosin either alone or with **Q2** (5 μM).

Figure 4. Porcine liver esterase-mediated hydrolysis of **Q2**. The stability of **Q2** (70 μM) in the presence porcine liver esterase (10 units/ml) at 37 ^{o}C was monitored by reverse phase HPLC using a Vydac C18 column with an eluent consisting of solvent A (H_2O/0.1% TFA) and solvent B (CH_3CN/0.1% TFA) with a 30 min gradient consisting of 5 to 50% A, a flow rate of 1 ml/min, and monitoring at 280 nm. Percent of **Q2** remaining was calculated based on the starting amount of **Q2**.

Downloaded from molpharm.aspetjournals.org at ASPET Journals on April 16, 2024

Molecular Pharmacology Fast Forward. Published on October 22, 2008 as DOI: 10.1124/mol.108.050492
This article has not been copyedited and formatted. The final version may differ from this version.

Figure 5. The ability of **Q2** and quinine to compete for the drug binding sites of P-gp was investigated using an [^{125}I]-IAAP photo-affinity labeling assay. (A) High Five crude membranes (25 μg) containing [^{125}I]-IAAP and increasing concentrations of quinine were photocrosslinked for 20 min on ice, subjected to separation by SDS-PAGE, and binding was visualized by autoradiography. Incorporation of IAAP into P-gp remained unchanged with various concentration of quinine. (B) Crude membranes (25 μg) containing [^{125}I]-IAAP and increasing concentrations of **Q2** were photocrosslinked for 20 min on ice, subjected to separation by SDS-PAGE, and binding was visualized by autoradiography. Incorporation of [^{125}I]-IAAP into P-gp was inhibited by **Q2** in a concentration-dependent manner. (C) Autoradiographs were analyzed by ImageJ. GF120918 (10 μM) was used as a positive control (A,B).

Figure 6. The effect of **Q2** on the basal (A) and verapamil-stimulated (B) ATPase activity of P-gp was assessed. High Five crude membranes (10 μg) vesicles incubated with or without verapamil (30 μM) and increasing concentrations of **Q2** were analyzed for ATPase activity by quantifying the amount of inorganic phosphate release spectrophotometrically. Cyclosporin A (10 μM) and quinine (25 μM) were used as controls.

Figure 7. Cellular viability of MCF-7/DX1 cells was evaluated using the MTT assay. A) Taxol dose-response curves obtained by the MTT assay after 72 h exposure in the absence or presence of increasing concentrations of **Q2**. B) **Q2** dose-response curve obtained by the MTT assay after 72 h exposure.

Downloaded from molpharm.aspetjournals.org at ASPET Journals on April 16, 2024

Molecular Pharmacology Fast Forward. Published on October 22, 2008 as DOI: 10.1124/mol.108.050492
This article has not been copyedited and formatted. The final version may differ from this version.

Table 1. IC_{50} values for monomeric and dimeric compounds obtained with the R123 accumulation assay using flow cytometric analyses. Dose-response curves were generated to determine the potency of the specified compounds. The parental MCF-7 cells were assayed as a negative control with and without inhibitors and verified that R123 readily accumulated in these cells and that fluorescence levels remained unchanged by co-incubation with the library members (data not shown).

	IC_{50} value of R123 accumulation assay[a] (μM)
Quinine	103
Quinidine	42
Q2	1.7
1	3.7
2	30
3	4.3
4	4.1
5	1.3
6	5.2

[a]IC_{50} values reported as half the maximum fluorescence level

Downloaded from molpharm.aspetjournals.org at ASPET Journals on April 16, 2024

Molecular Pharmacology Fast Forward. Published on October 22, 2008 as DOI: 10.1124/mol.108.050492
This article has not been copyedited and formatted. The final version may differ from this version.

Table 2. MCF-7 and MCF-7/DX1 cytotoxicity IC_{50} values for taxol with various concentrations of co-administered **Q2**. IC_{50} values reported as the concentration leading to 50% of cell viability. Cellular viability as measured by the MTT assay following a 72 h incubation with the specified compounds. IC_{50} values reported as the concentration leading to 50% of cell viability. N/A, not available.

	Taxol in the presence of Q2				
	Q2 0 μM	**Q2 1 μM**	**Q2 2 μM**	**Q2 4 μM**	**Q2 6 μM**
MCF-7	3.1 ± 1.0 nM	N/A	N/A	N/A	N/A
MCF-7/DX1	9.03 ± 0.03 μM	6.3 ± 0.2 μM	2.0 ± 0.3 μM	3.0 ± 1.1 nM	4.0 ± 1.0 nM

Downloaded from molpharm.aspetjournals.org at ASPET Journals on April 16, 2024

Figure 1

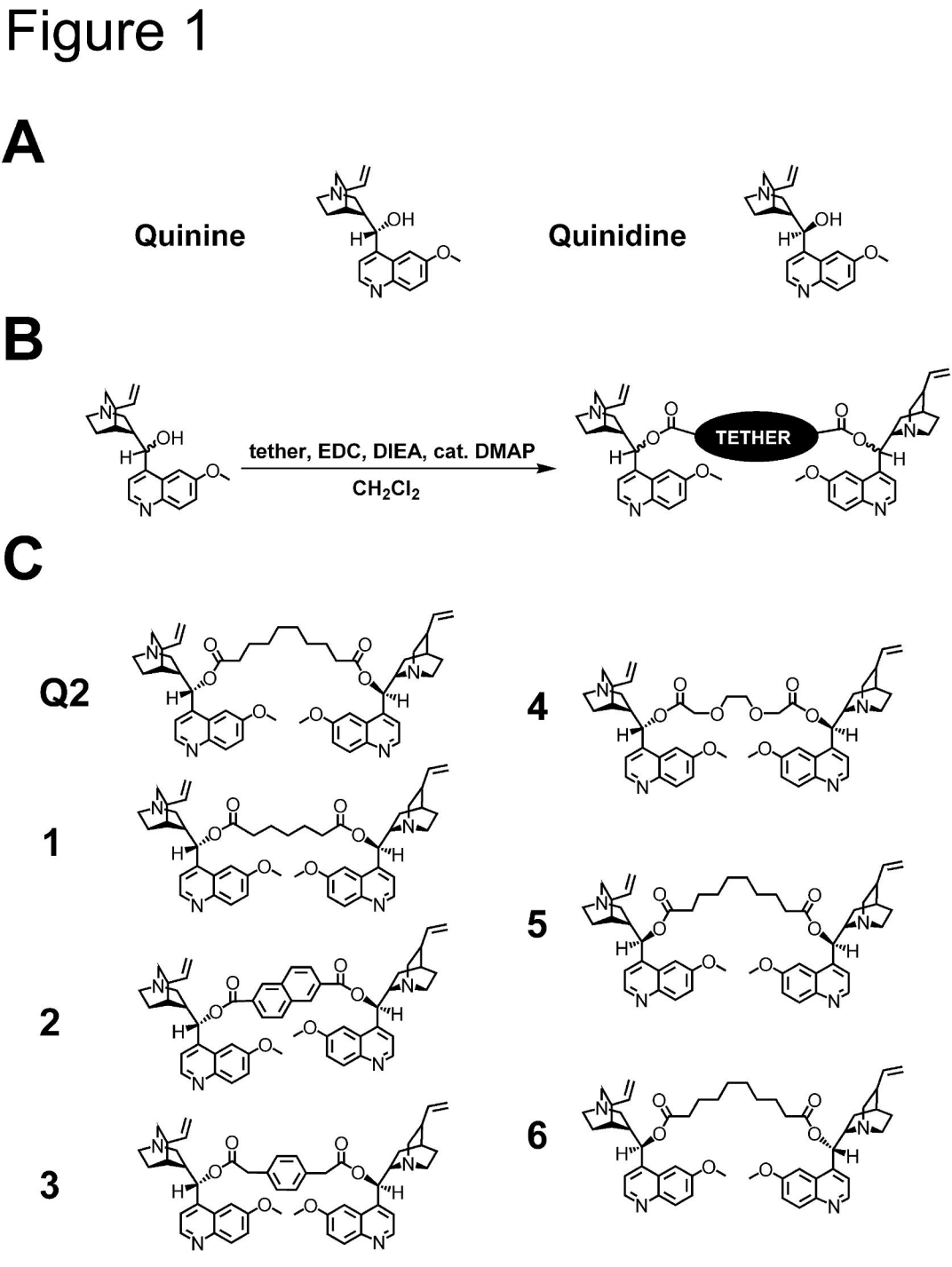
A
Quinine
Quinidine
B
tether, EDC, DIEA, cat. DMAP
CH2Cl2
TETHER
C
Q2
1
2
3
4
5
6

Figure 2

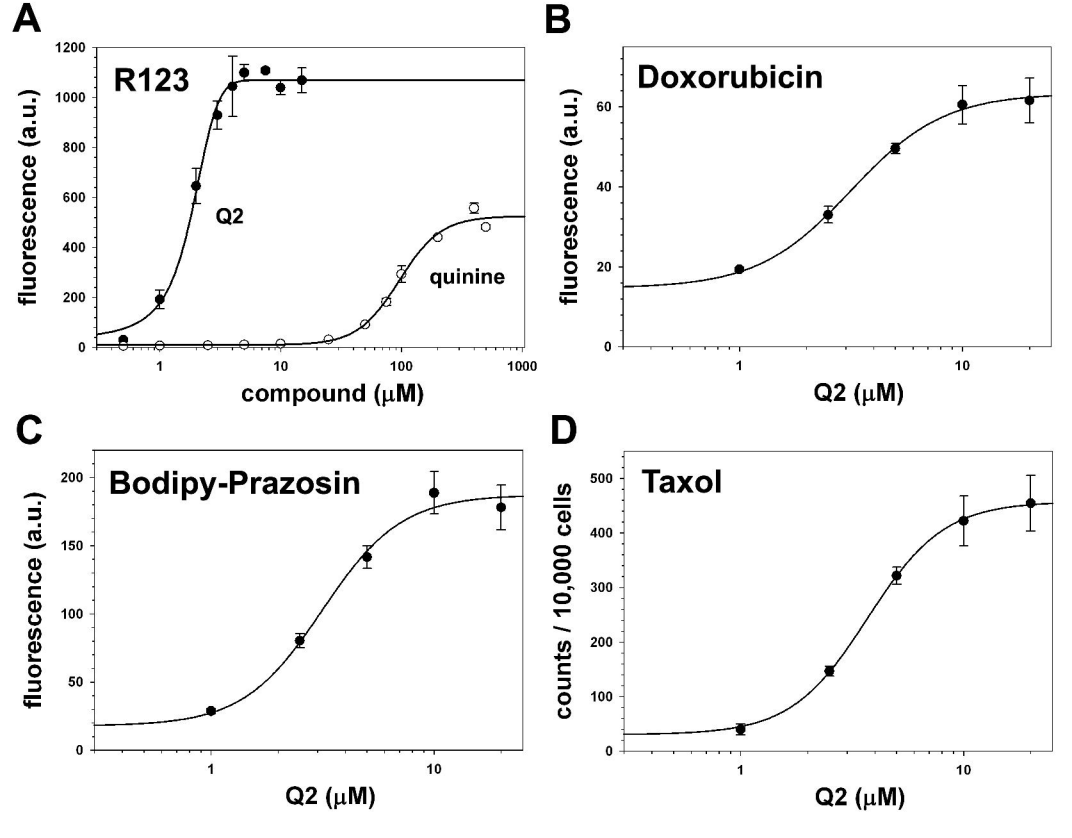
A
R123
Q2
quinine
fluorescence (a.u.)
compound (μM)
B
Doxorubicin
fluorescence (a.u.)
Q2 (μM)
C
Bodipy-Prazosin
fluorescence (a.u.)
Q2 (μM)
D
Taxol
counts / 10,000 cells
Q2 (μM)

Figure 3

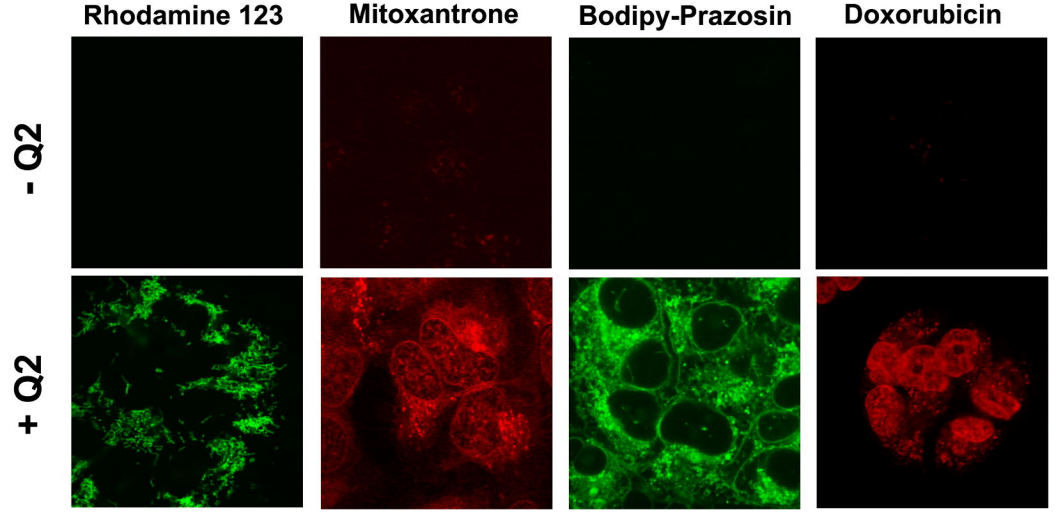
Rhodamine 123
Mitoxantrone
Bodipy-Prazosin
Doxorubicin
- Q2
+ Q2

Figure 4

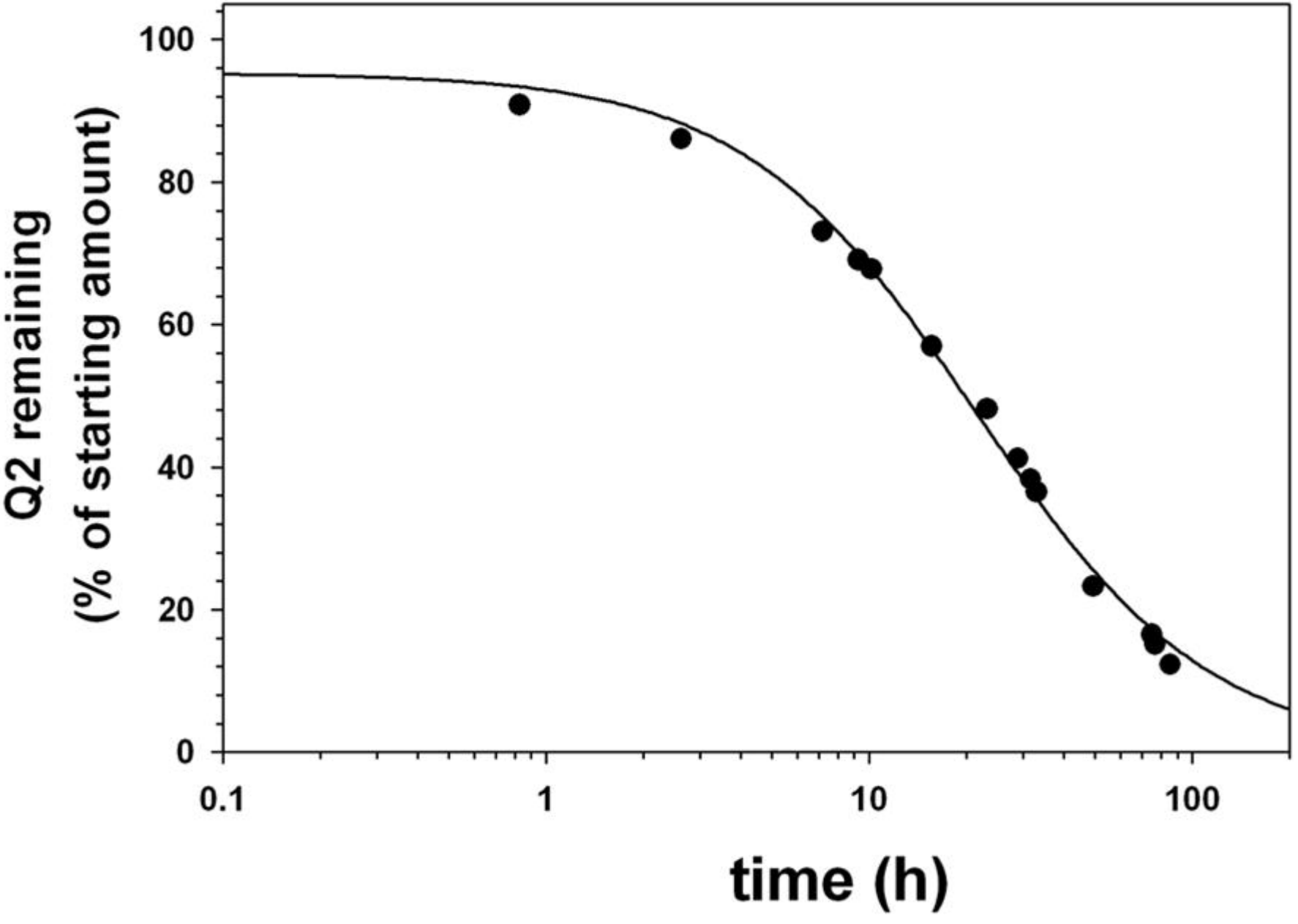
Q2 remaining
(% of starting amount)
100
80
60
40
20
0
0.1
1
10
100
time (h)

Figure 5

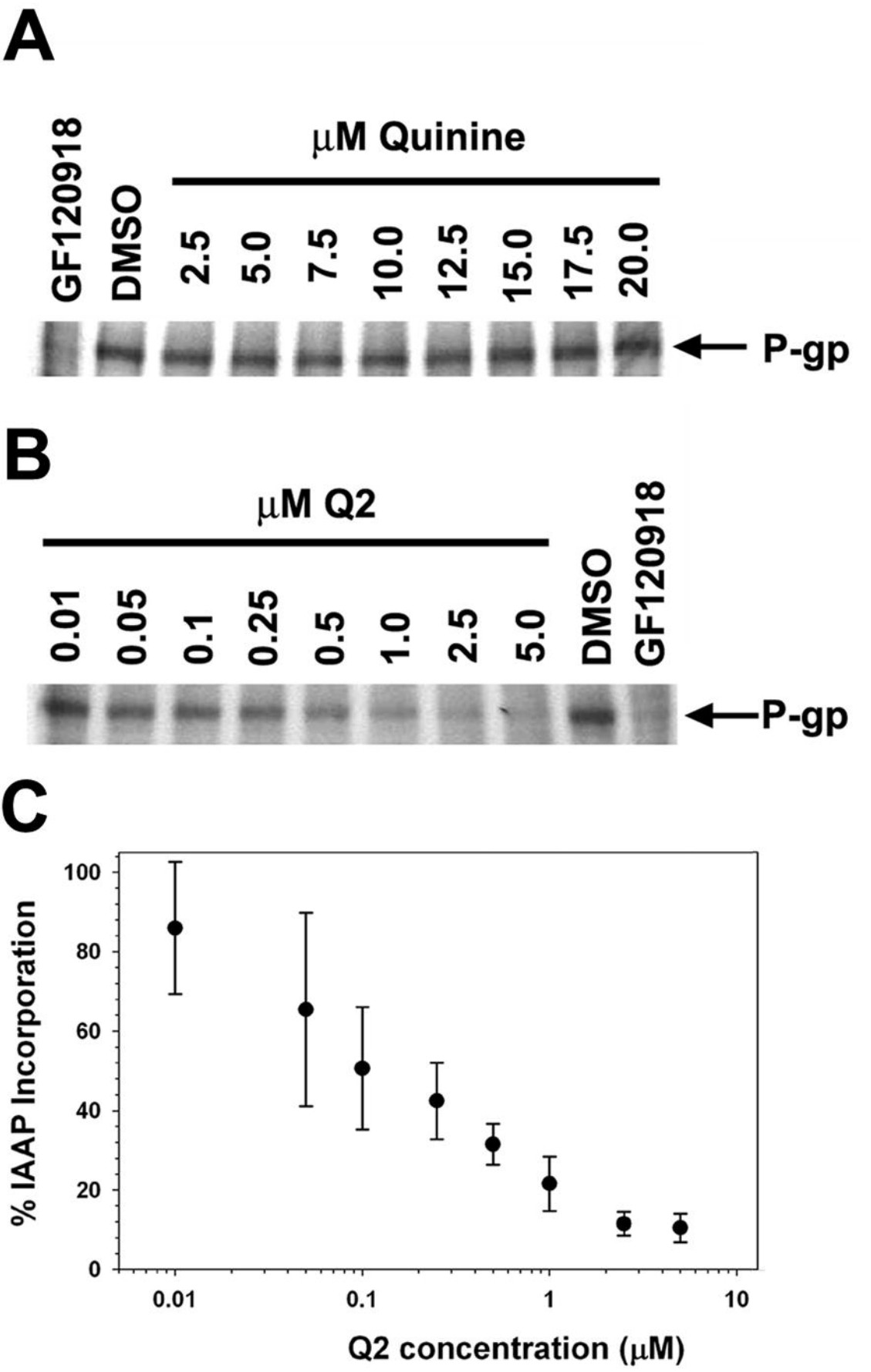
A
μM Quinine
GF120918
DMSO
2.5
5.0
7.5
10.0
12.5
15.0
17.5
20.0
P-gp
B
μM Q2
0.01
0.05
0.1
0.25
0.5
1.0
2.5
5.0
DMSO
GF120918
P-gp
C
% IAAP Incorporation
100
80
60
40
20
0
0.01
0.1
1
10
Q2 concentration (μM)

Figure 6

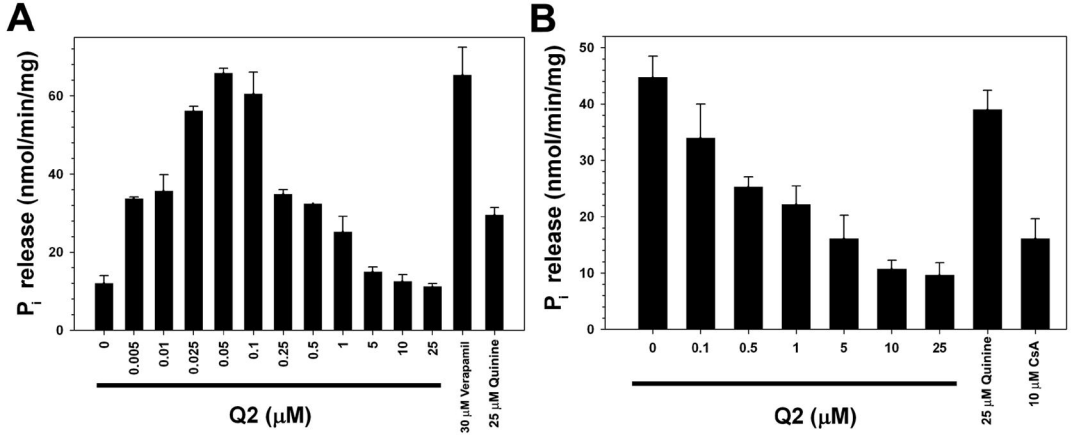
A
P_i release (nmol/min/mg)
0
20
40
60
0
0.005
0.01
0.025
0.05
0.1
0.25
0.5
1
5
10
25
30 μM Verapamil
25 μM Quinine
Q2 (μM)
B
P_i release (nmol/min/mg)
0
10
20
30
40
50
0
0.1
0.5
1
5
10
25
25 μM Quinine
10 μM CsA
Q2 (μM)

Figure 7

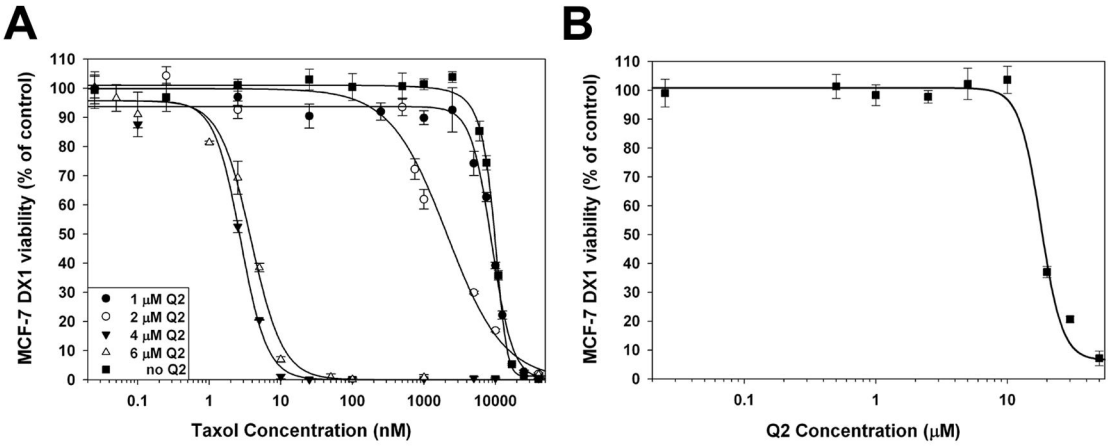
A
B
MCF-7 DX1 viability (% of control)
Taxol Concentration (nM)
1 μM Q2
2 μM Q2
4 μM Q2
6 μM Q2
no Q2
Q2 Concentration (μM)